

## Construction and Evaluation of Molecular Models: Guide and Design of Novel SE Inhibitors

Yunfei An, Yue Dong, Liu Min, Liyu Zhao, Dongmei Zhao, Jun Han, and Bin Sun\*

Cite This: <https://dx.doi.org/10.1021/acsmmedchemlett.0c00017>

Read Online

ACCESS |

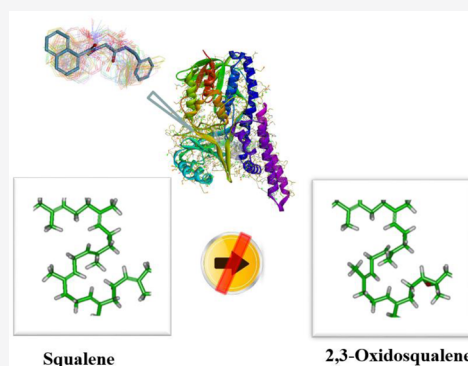
Metrics &amp; More

Article Recommendations

Supporting Information

**ABSTRACT:** Squalene epoxidase (SE) was considered an important antifungal target to block ergosterol synthesis. In this study, molecular models of CASE including the homology model and the SBP were constructed, respectively. Three representative SE inhibitors were selected and docked into the active site of CASE. Subsequently, the novel SE inhibitors were designed based on the analysis of the inhibitor binding mode and the distribution of pharmacophore features. These compounds were further synthesized and tested *in vitro*. They exhibited a certain degree of antifungal activity, especially compound 7a-2, which also has a significant inhibitory effect on resistant fungi. Further analysis found that compound 7a-2 could inhibit SE, which is similar to naftifine. The study proved the rationality of the molecular models; they can help us design and discover more potent antifungal SE inhibitors.

**KEYWORDS:** Fungal infections, homology model, SE inhibitors, antifungal activity



In recent years, with the abuse of immunosuppressive agents and broad-spectrum antibiotics in the clinic, fungal infection has increased dramatically.<sup>1,2</sup> At the same time, it also shows a trend of more and more difficult treatment, especially the increase in immunocompromised patients and the emergence of drug-resistant pathogenic fungi. Fungal infection is becoming a serious threat to human health.<sup>3</sup> Clinically, the pathogens of most fungal infections are the *Aspergillus spp.*, *Cryptococcus spp.*, and *Candida spp.*, especially of *Candida albicans*, which accounted for 51.9% in the fungal infections of blood.<sup>4,5</sup> Therefore, it is an urgent task to discover the novel highly effective antifungal agents.

At present, the different kinds of antifungal agents, which include the antimetabolites, polyenes, and azoles, have been widely used in clinical practice.<sup>6–9</sup> However, they also have many defects, such as low bioavailability, liver toxicity, and drug resistance.<sup>10</sup> It is worth noting that allylamine antifungal agents (e.g., naftifine, terbinafine) as representative SE inhibitors have the advantages of low toxic side effects and low resistance (Figure 1).<sup>11</sup> Ergosterol can maintain the permeability and fluidity of fungal cell membranes; the allylamine antifungal agent can block the ergosterol synthesis by inhibiting SE activity and cause the accumulation of squalene.<sup>12,13</sup> The lack of ergosterol can destroy the structure of fungal cell membranes.<sup>14</sup> Finally, these inhibitors can produce the dual effects of bactericidal and bacteriostatic. However, these SE antifungal inhibitors also have some other problems that need to be solved, such as single structure, low bioavailability, and narrow antifungal spectrum.<sup>15,16</sup> Therefore, it is very important to discover the novel SE antifungal

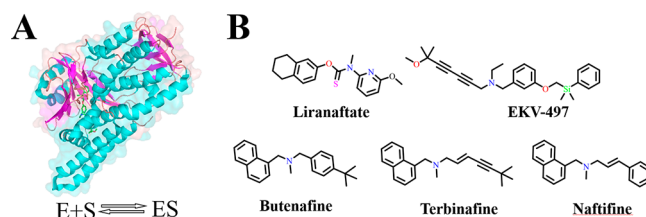


**Figure 1.** (A) Crystal structure of SE protein (*Homo sapiens*); (B) Representative SE inhibitors with various chemical scaffolds.

inhibitors with broad spectrum, potent activity, and low resistance.

At present, the crystal structure of CASE has not been resolved.<sup>17–19</sup> Therefore, the CASE homology model needs to be constructed, and it can provide the important guidance for designing novel antifungal SE inhibitors. First, the amino acid sequence of CASE was searched through the UniProtKB/Swiss-Prot, and its accession number is Q92206, which contains 496 amino acid residues. Subsequently, the homology template of CASE was determined with BLAST.

The result is shown in Table 1. It can be seen that squalene epoxidase (SE) of *Homo sapiens* (PDB code: 6C6N) with

**Received:** January 11, 2020

**Accepted:** May 11, 2020

**Published:** May 11, 2020

Table 1. BLAST Results of CASE

Name	Species source	Identity	Resolution	Score	V-value	PDB code
Q92206	<i>Homo sapiens</i>	41.59	2.3 Å	750	$1.6 \times 10^{-92}$	6C6N
Q9HWJ1_PSEAE	<i>Pseudomonas aeruginosa</i>	21.3	1.75 Å	133	$5.8 \times 10^{-8}$	2X3N
TETX_BACT4	<i>Bacteroides thetaiotaomicron</i>	22.4	2.09 Å	110	$3.7 \times 10^{-5}$	2XDO
Q93LY7_9ACTN	<i>Streptomyces sp. PGA64</i>	23.8	1.8 Å	104	$2.3 \times 10^{-4}$	2QA1
Q4KCZ0_PSEFS	<i>Pseudomonas fluorescens</i>	22.1	2.75 Å	102	$3.8 \times 10^{-4}$	SDBJ



Figure 2. Result of sequence alignment of Q92206 (CASE) and 6C6N. Semiconserved constitution, blue; Conserved constitution, deep blue.

cocrystallized ligand (EKV497) possesses the highest scoring values (750) and sequence similarity (Identity: 41.59%).<sup>20</sup> Therefore, 6C6N was selected as template protein (Figure 2). The CASE homology model was built, and the cocrystalline ligand-EKV497 was retained to construct the active site. Five CASE homology models were generated.

The function values can directly reflect the properties of the homology model. The result of Table 2 shows the homology

Table 2. Detailed Summary of Homology Model Scores

CASE Model	PDF Physical Energy	PDF Total Energy	DOPE Score
CASE.M0003	1880.19	3989.16	-53188.84
CASE.M0005	1895.00	4061.91	-54293.64
CASE.M0004	1892.16	4086.41	-53378.76
CASE.M0002	2000.30	4260.59	-52937.94
CASE.M0001	2052.41	4341.68	-52695.61

model CASE.M0003 with the lowest scores (PDF Physical Energy: 1880.19, PDF Total Energy: 3989.16, DOPE Score: -53188.84) was selected as the best homology model. At the same time, it can also show the best match with the template protein 6C6N (Supporting Information, Figure 2).

Subsequently, the rationality of the CASE.M0003 model was analyzed and verified through the Ramachandran plot (Figure 3A and Table 3).<sup>21,22</sup> These amino acid residues account for 99.1%, which are distributed in the favored regions and allowed regions. The other residues (Glu 131, Arg 132, Asp 275, and Lys 318) in the unallowed region account for 0.9%; they are located on the protein surface and far away from the active site. In order to further investigate the compatibility between residues of the CASE.M0003 model, Verify 3D was performed, and the result was shown in the Profile-3D plot (Figure 3B). 95.37% of the amino acid residues with Verify

score is above 0, which represents that these main amino acids are in a reasonable position. In addition, a few amino acid residues (4.63%) were located in the tail and trans membrane regions (<0), which has low influence on the follow-up study. The verify score of the CASE homology model is 186.88, and it has a small gap with the expected verification high value (225.23). Therefore, the CASE.M0003 model is a reasonable choice.

The CASE.M0003 provides an intuitive perspective to analyze the active site, which was shown in Figure 4. The active pocket can be divided into regions A and B according to the binding mode of the ligand molecule (EKV-497). One nonionized polar amino acid residues (Tyr251) and five hydrophobic residues (Leu 48, Val 240, Leu 249, Leu 340, and Leu 434) are distributed in binding region A. Moreover, there are three hydrophobic residues (Cys 416, Phe 420, and Phe 448) around region B. Further analysis found that the ligand molecule (EKV-497) is bound in the active site of CASE. The aromatic group of EKV-497 can form the  $\pi$ -alkyl interaction with the key hydrophobic residues (Leu48, Val240, Tyr251, and Leu340) in region A. At the same time, the 2-methoxyisopropyl group is positioned in the bottom region B, and it can form the hydrophobic interaction with Phe 448.

In order to study the binding mode of SE inhibitors, three representative allylamine compounds (naftifine, terbinafine, and butenafine) were selected and docked into the active site;<sup>23,24</sup> the result was shown in Table 4. It can be seen that their docking energy values are below 0 (CDOCKER INTERACTION ENERGY: -35.77, -29.14, -33.62 kcal/mol; CDOCKER ENERGY: -4.64, -3.97, -4.45 kcal/mol), which suggests these compounds can produce strong binding energy with the target enzyme CASE. It is worth noting that naftifine with the lowest CDOCKER energy value can be properly docked into the SE active site, which indicated that its

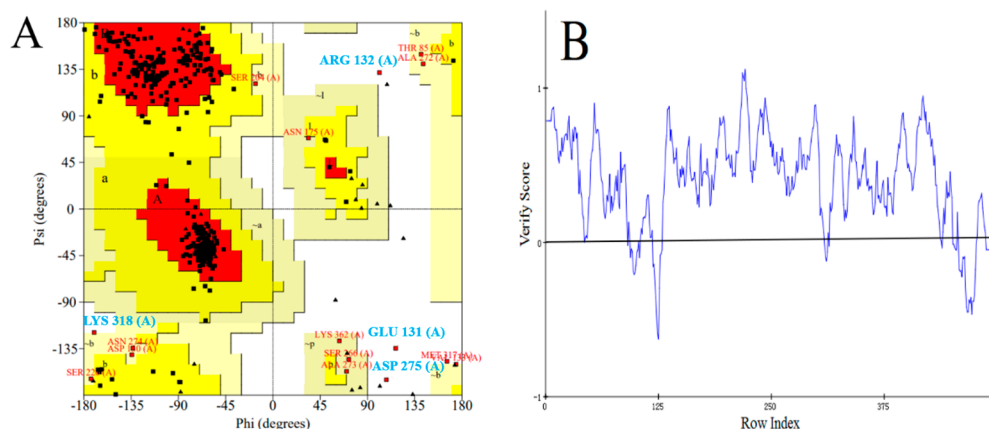


Figure 3. (A) Evaluation of the CASE.M0003 model by Ramachandran plot. (B) Evaluation of the CASE.M0003 model by Profile-3D plots.

Table 3. Ramachandran Plot

Disallowed regions	Generously allowed regions	Additional allowed regions	Most favored regions
0.9%	5.9%	28.5%	64.7%

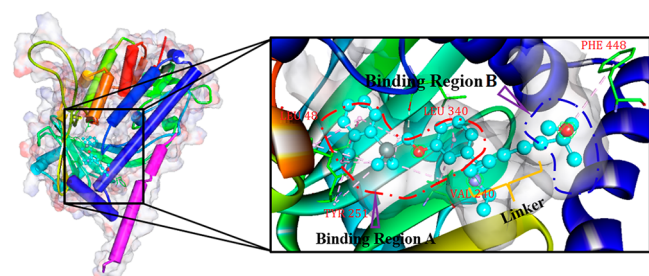


Figure 4. Three-dimensional representation of CASE.M0003 associated with ligand EKV-497.

Table 4. Docking Studies of Three Representative Allylamine Drugs

Name	-CDOCKER INTERACTION ENERGY	-CDOCKER ENERGY	Bond Energy
Naftifine	35.77	4.64	1.46
Terbinafine	29.14	3.97	2.31
Butenafine	33.62	4.45	1.41

core groups can produce the most stable interaction with CASE.

Those key amino acid residues (Tyr 77, Val 240, Leu 249, Leu 340, Leu 394, Leu 398, Phe 402, Cys 416, Phe 420, Pro 430, Leu 434, and His 447) are distributed around the allylamine compounds (Figure 5). Their naphthyl group is bound in region A and forms the  $\pi$ -alkyl and  $\pi$ - $\pi$  interactions with the residues (Tyr 77, Leu 340, and Phe 402). The struct phenyl or *tert*-butyl structure of SE inhibitors is bound to the active region B, and they can produce the  $\pi$ -alkyl interaction with surrounding residues (Leu 398, Cys 416, and Pro 430). It is worth noting that the binding ability of the phenyl group is better than that of the *tert*-butyl group. The flexible branch is located between the naphthyl and phenyl groups, which can play an important linking role.

Pharmacophore model is a summary of inhibitor characteristics, and its features can directly reflect the binding conformation of SE inhibitors. Therefore, the SBP was further constructed to study the binding characteristics of SE

inhibitors with target enzyme.<sup>25</sup> In this study, the CASE.M0003 with docking molecule (naftifine) was selected as the research object. First, the pharmacophore feature set is obtained by analyzing the interaction between the ligand molecule (naftifine) and the SE receptor, which is shown in Figure 6A. The hydrophobic features (H) occupy the dominant position; they are positioned in the central region of the active cavity, and some of the hydrogen bond donor or acceptor features are distributed outside the region. Then, the pharmacophore feature set was further classified and clustered. The core feature information was determined by analyzing the characteristics of the binding site (Figure 6B).

Finally, the SBP was composed with three hydrophobic features (H<sub>1</sub>, H<sub>2</sub>, and H<sub>3</sub>) and some exclusion volume, and these features can match on the core fragment groups of naftifine. We can see that the hydrophobic features (H<sub>1</sub> and H<sub>2</sub>) were bound to the naphthyl group, and they are located in active region A. In addition, the hydrophobic features (H<sub>3</sub>) were positioned at the phenyl group in the active region B. The result indicates that the core groups of naftifine play an important role in antifungal activity (Figure 7A, B).

In the design process for novel SE inhibitors, the naphthyl and phenyl groups of naftifine were retained, which are superimposed on specific pharmacophore features. Subsequently, they were connected by a flexible branched chain (Figure 8A), the novel SE inhibitor was constructed, and its structure was modified and optimized as the leading compound, which was shown in Figure 8B. The drugability of these target compounds was further analyzed to improve the success rate. Their molecular weight is less than 500, the number of rotatable bonds is 6, the hydrogen bond acceptors, hydrogen bond donor, and lipid-water partition coefficients are all less than 5. The properties of these designed compounds were in line with the Lipinski's rule of five. Finally, they were identified for subsequent studies.

Their synthetic route is shown in Scheme 1. L-Glycine (2) as the starting material can form glycine ethyl ester hydrochloride (3) by formylation. Next, the amino acid ester hydrochloride was separately treated with the different aromatic carboxylic acids (1a–d) to generate the corresponding key intermediates (4a–d). Subsequently, the methyl group was introduced into these intermediates to give the required products (5a–d) through methylation reaction. They were further hydrolyzed to generate the intermediate organic acids (6a–d) in alkaline conditions. Finally, the target compounds 7a–d-1, 2 were obtained via amidation reaction.

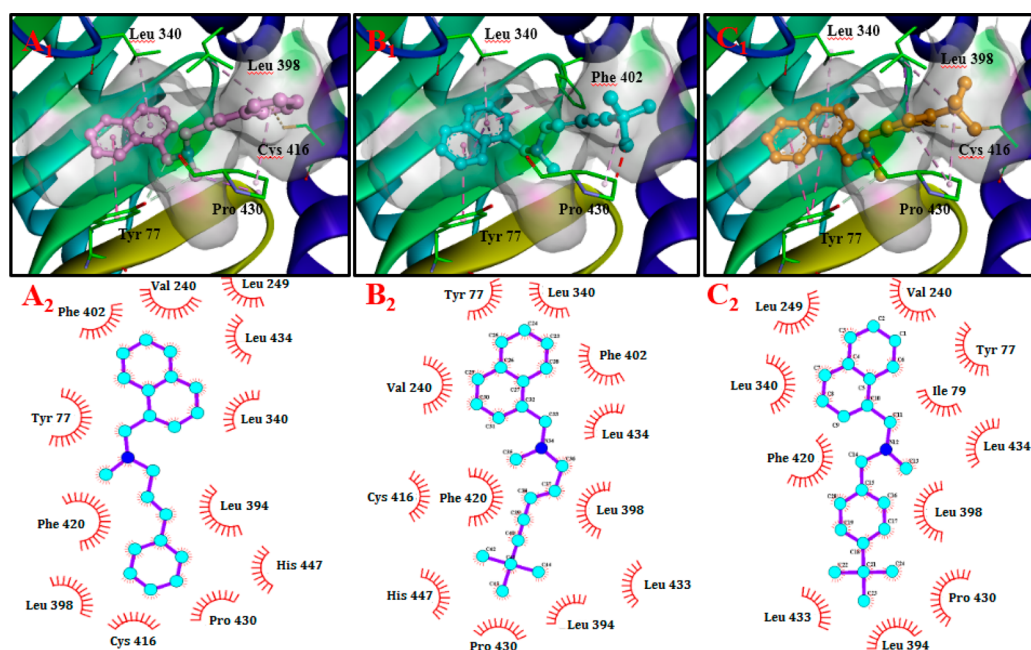


**Figure 5.** Docking models of representative allylamine drugs (naftifine, terbinafine, and butenafine). (A<sub>1</sub>) The interaction of naftifine in the active site of CASE.M0003. (A<sub>2</sub>) The interaction between the CASE.M0003 and naftifine on 2D diagram. (B<sub>1</sub>) The interaction of terbinafine in the active site of CASE.M0003. (B<sub>2</sub>) The interaction between the CASE.M0003 and terbinafine on 2D diagram. (C<sub>1</sub>) The interaction of butenafine in the active site of CASE.M0003. (C<sub>2</sub>) The interaction between the CASE.M0003 and butenafine on the 2D diagram.

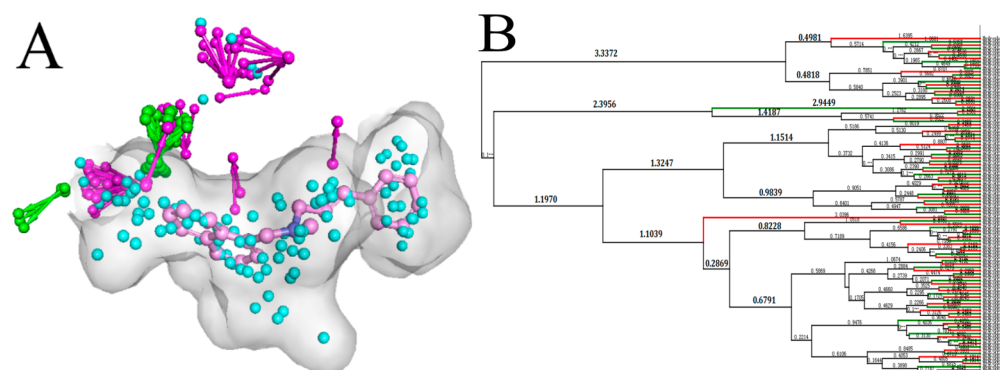


**Figure 6.** (A) Location of the different pharmacophore features. Hydrophobic: cyan; Acceptor: green; Donor: purple. (B) Clustering of hydrophobic feature groups.

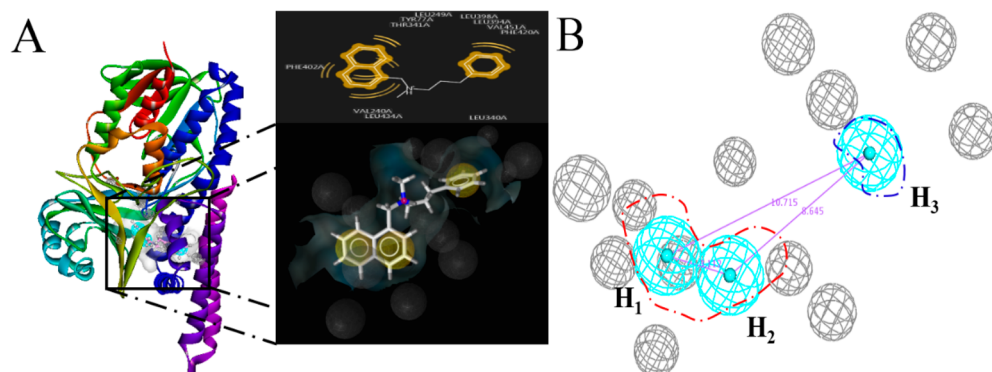


**Figure 7.** (A) The matching results of naftifine and pharmacophore features. (B) The features distribution of SBP in the binding region of CASE.

Their biological activity *in vitro* was evaluated through the protocols of NCCLS.<sup>26,27</sup> Naftifine was identified as the positive control drug, and test strains included four pathogenic *Candida* spp. (*C. alb.*; *C. tro.*; *C. gla.*; *C. kru.*) and one

*Aspergillus* spp. (*A. fum.*). The result was summarized, and it was shown in Table 5. Most compounds displayed a certain degree of antifungal activity against different fungal strains. It was observed that the target compounds 7b-1, 7b-2, 7c-1, and

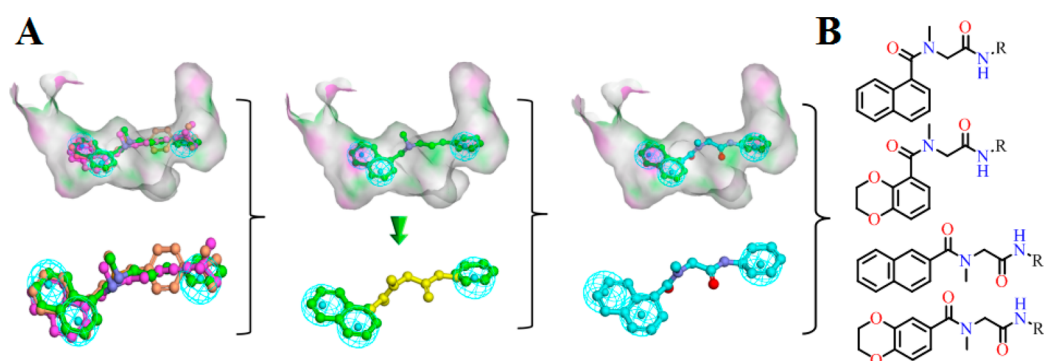
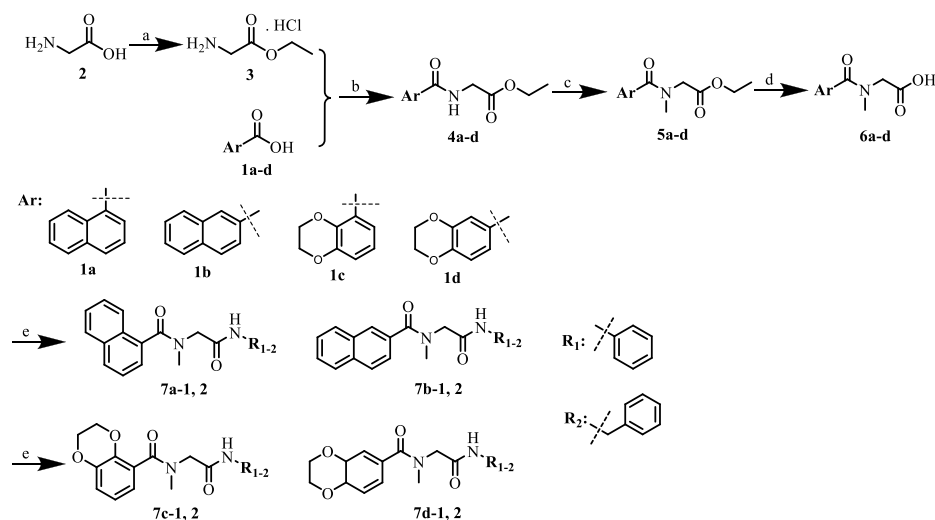


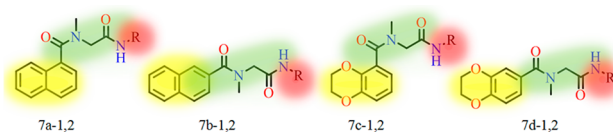
**Figure 8.** (A) The design of novel SE inhibitors by analyzing the binding model of naftifine. (B) The structural characteristics of novel SE inhibitors.

**Scheme 1**<sup>a</sup>



<sup>a</sup>Reagents and conditions: (a)  $\text{SOCl}_2$ , ethanol, 65 °C, 6 h; (b) HOBt, EDCl, DIEA, 80 °C, 7 h; (c)  $\text{CH}_3\text{I}$ ,  $\text{K}_2\text{CO}_3$ , THF, 60 °C, 5 h; (d) methanol, 2 N sodium hydroxide solution, 65 °C, 2 h; (e) HATU, DIEA, amine (aniline or benzylamine), DMF, 80 °C, 7 h.

**Table 5. Summary of Biological Activity against Different Pathogenic Fungi<sup>a</sup>**



Compd	R	MIC, $\mu\text{g}/\text{mL}$				
		<i>C. alb.</i>	<i>C. tro.</i>	<i>C. gla.</i>	<i>C. kru.</i>	<i>A. fum.</i>
7a-1	aniline	0.25	0.5	0.5	0.25	8.0
7a-2	phenylmethanamine	0.125	0.5	0.25	0.125	4.0
7b-1	aniline	0.5	0.5	2.0	1.0	>16
7b-2	phenylmethanamine	0.5	0.25	0.25	0.5	8.0
7c-1	aniline	0.5	1.0	1.0	0.5	>16
7c-2	phenylmethanamine	0.25	0.5	0.25	0.25	8.0
7d-1	aniline	1.0	0.5	0.5	2.0	8.0
7d-2	phenylmethanamine	0.5	0.5	2.0	0.5	>16
Naftifine		0.5	0.5	0.5	1.0	>16

<sup>a</sup>Abbreviations: *C. alb.*, *Candida albicans* (ATCC 10231); *C. tro.*, *Candida tropicalis* (ATCC 1369); *C. gla.*, *Candida glabrata* (ATCC 0001); *C. kru.*, *Candida krusei* (ATCC 6258); *A. fum.*, *Aspergillus fumigatus* (KM8001).

**7d-2** can inhibit the *C. alb.* and *C. tro.* with MIC value in the range (0.5–2  $\mu\text{g}/\text{mL}$ ), and the antifungal effect is similar to the reference drug (naftifine). In addition, compounds **7a-1**

and **7c-2** also showed the excellent antifungal activity on *Candida spp.*, but their inhibitory activity against *A. fum.* is not ideal. Interestingly, the antifungal activity of compounds **7a-2**

with MIC value in the range (0.125–4  $\mu\text{g}/\text{mL}$ ) displayed the broader antimicrobial spectrum than other compounds; it can inhibit the activity of *Candida. pp.* and *A. fum.* In summary, these target compounds can maintain the antifungal activity, and their fragment groups can lead to some of the change in biologic activity and antifungal spectrum.

Fluconazole, as a representative antifungal drug, has been widely used in clinical antifungal treatment, and it achieved good therapeutic effect. However, the more and more pathogenic fungi have developed the phenomenon of drug resistance with the increase of clinical treatment time. Therefore, it is of important significance to evaluate the antiresistant fungal activity of these compounds. The preferred compounds (7a-1, 7a-2, and 7c-2) were selected, and their antifungal activity is summarized in Table 6. The target

**Table 6. Anti-Fluconazole Resistant Fungal Activity of the Preferred Compounds *in Vitro***

Compd	MIC, $\mu\text{g}/\text{mL}$				
	Strain CaR	Strain 17#	Strain 901	Strain 632	Strain 904
7a-1	8	>16	4	>16	>16
7a-2	4	4	4	8	>16
7c-2	4	>16	>16	>16	8
Naftifine	4	8	>16	8	8
Fluconazole	>16	>16	>16	>16	>16

<sup>a</sup>Abbreviations: Strain CaR, Strain 17#, Strain 901, Strain 632, and Strain 904, fluconazole-resistant strains of *Candida albicans*. These strains were provided by Shenyang Pharmaceutical University.

compounds 7a-1 and 7c-2 with MIC values > 16  $\mu\text{g}/\text{mL}$  did not demonstrate the significant inhibitory activity against the strains 17# and Strain 632, which was isolated from AIDS patients. It was worth noting that compound 7a-2 with MIC value 4  $\mu\text{g}/\text{mL}$  showed moderate inhibitory activity against Strain 17#, Strain CaR, and Strain 901.

Fungal cell density is an important index, which can directly reflect their growth status. In this study, the different concentrations (0 nmol/mL, 50 nmol/mL and 5 nmol/mL) of naftifine and compound 7a-2 were set in the solution of *C. alb.*

We can see that fungal cell displayed the proliferation ability at the concentration of 0 nmol/mL, and some fungal cells display the phenomenon of spore proliferation in the solution; their cell density is significantly higher than the other concentration groups (Figure 9 A<sub>1, 2-1</sub>). In the high and low concentration treated groups (50 nmol/mL, 5 nmol/mL) with compound 7a-2 and naftifine, the cell proliferation of *C. alb.* was inhibited, and their cell density decreased significantly compared with the untreated group (Figure. 9A<sub>1, 2-2, 3</sub>). Subsequently, TEM was further performed to observe the cell morphological changes of *C. alb.* In the early stage, the fungal cell showed the elliptical structure, their nucleus and organelles were distributed in the center of cells, and the cell wall and membrane structure were covered on the cell surface. It is worth noting that some fungal cells show a tendency to divide. With the prolonged treatment of fungal cells with compound 7a-2, the phenomenon of fungal cell division disappeared, and the structure of cell walls and cell membranes began to become uneven. At the same time, some fungal cells showed internal material exuding from the cells (Figure

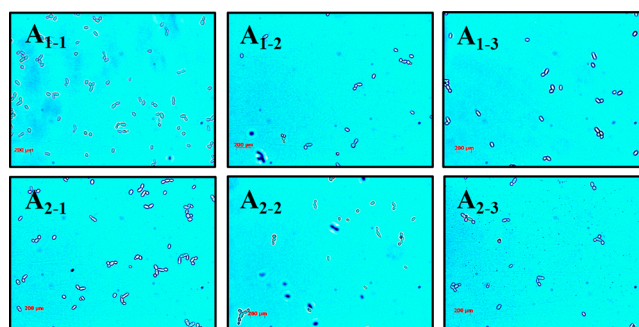


**Figure 9.** Changes of fungal cell (*C. alb.* ATCC SC5314) density were observed in different concentrations (A<sub>1, 2-1</sub>: 0 nmol/mL; A<sub>1, 2-2</sub>: 50 nmol/mL; A<sub>1, 2-3</sub>: 5 nmol/mL). A<sub>1-1, 2, 3</sub>: Treated with naftifine; A<sub>2-1, 2, 3</sub>: Treated with compound 7a-2.

10B<sub>1, 2</sub>). The result indicated that the compound has destroyed the external structure of the fungal cells.

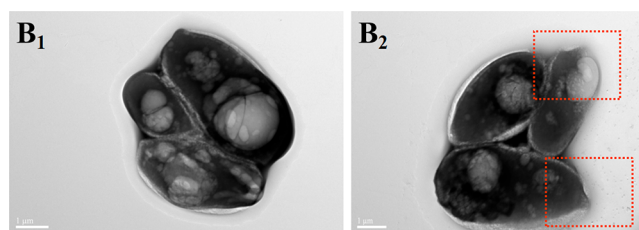


**Figure 10.** Transmission electron microscopy (TEM) results. B<sub>1</sub>: Untreated; B<sub>2</sub>: Treated with compound 7a-2.

It was an important condition for drugability to investigate the stability of the compound in plasma. In this study, compounds 7a-2 and 7c-2 with higher antifungal activity were selected to be incubated with human plasma, which was shown in Table 7; we can see that they exhibit high stability at 120 min (remaining 91.6% and 83.5%, respectively).

**Table 7. Stability of Target Compounds 7a-2 and 7c-2**

Compd.	% Incubating for 60 min	% Incubating for 120 min
7a-2	94.5	91.6
7c-2	87.3	83.5

LC-MS was performed to study the change of sterol composition in different treatment groups; the result was summarized in Table 8. It can reflect the biological mechanism of compound 7a-2.<sup>28,29</sup> In the blank control, ergosterol was the dominant component, which contained 96.7%, while eburicol only accounted for 1.2%. At the same time, there is no squalene in this component. When the *C. alb.* were treated with different concentrations of naftifine and compound 7a-2 (0.125–4  $\mu\text{g}/\text{mL}$ ), the proportion of ergosterol in the cell membrane decreased to 28.4% and 31.7% from 96.7%, and the contents of squalene, eburicol, and unknown sterol were accumulated. In particular, the content of squalene increased sharply to 64.5% and 58.9%, respectively. Therefore, they showed the same changing trend of ergosterol and squalene. The possible reason was that ergosterol synthesis was blocked by inhibiting the target enzyme SE.

Molecular docking can guide the design and optimization of target compounds by determining the binding mode of molecules. The target compound 7a-2 and naftifine with

Table 8. Change of Sterol Composition in Different Conditions

Compd.	Concentration ( $\mu\text{g/mL}$ )	% of total sterols ( <i>C. alb.</i> )			
		Ergosterol	Squalene	Eburicol	Unknown sterol
7a-2	0.125	87.4	9.8		2.8
	0.5	63.9	29.5	1.6	5.0
	4	31.7	58.9	2.3	7.1
Naftifine	0.125	83.6	14.8		1.6
	0.5	62.9	31.5	0.7	4.9
	4	28.4	64.5	1.7	5.4
Control		96.7		1.2	2.1

pharmacophore features were bound to the active site of CASE, respectively. As shown in Figure 11A–C, compound

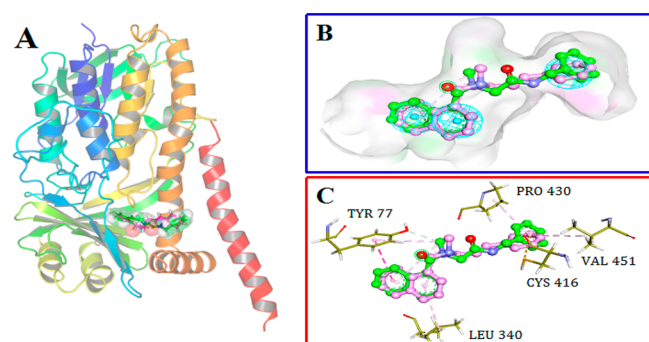


**Figure 11.** (A) Molecular docking of target compound 7a-2 and naftifine with target enzyme (CASE). (B) The common feature pharmacophore model matching compound 7a-2 and naftifine in the active site. (C) The interaction of this docking molecule (compound 7a-2, naftifine) with the target enzyme (CASE). Compound 7a-2 is shown as green rod-shaped structure; naftifine is shown as pink rod-shaped structure.

7a-2 and naftifine exhibit the same binding conformation and action mode. Their phenyl groups were combined in the upper region of the active site, and it can match with the hydrophobic feature ( $H_3$ ). The  $\pi$ -alkyl and  $\pi$ - $\pi$  interaction were generated between the hydrophobic residues (Val 451, Pro 430) and the phenyl group. In addition, the 1-naphthyl group with the hydrophobic features ( $H_1$ ,  $H_2$ ) binds in the bottom region; it can form the hydrophobic interactions ( $\pi$ -alkyl and  $\pi$ - $\pi$ ) with the surrounding key residues (Tyr 77, Val 240, and Leu 340).

In conclusion, the homology model (CASE.M0003) was constructed with the high homology *Homo sapiens* squalene epoxidase as template. At the same time, the reliability and compatibility of the model were further evaluated through the methods of Ramachandran plots and Verify 3D. Three representative SE inhibitors (naftifine, terbinafine, butenafine) were selected and docked into the target enzyme CASE, and the naftifine with the highest docking value can form the stable binding effect. Subsequently, the SBP was further constructed by analyzing the binding conformation of SE inhibitors, which contains three hydrophobic (H) features. On this basis, the novel target compounds as SE inhibitors were designed, synthesized, and tested *in vitro*. They exhibited the difference of antifungal activity. Among these, compound 7a-2 not only showed an excellent antifungal activity against the different strains but also a significant inhibitory effect on resistant fungi. Notably, compounds 7a-2 and 7c-2 also exhibited blood plasma stability. Further analysis found that compound 7a-2 could block the synthesis of ergosterol by inhibiting CASE,

which is similar with the mechanism of naftifine. The study proved a guide to design and discovery of novel target compound.

## ■ ASSOCIATED CONTENT

### Supporting Information

The Supporting Information is available free of charge at <https://pubs.acs.org/doi/10.1021/acsmchemlett.0c00017>.

The general methods for organic synthesis, biological evaluation, and model construction; the structure spectra of target compound. (PDF)

## ■ AUTHOR INFORMATION

### Corresponding Author

**Bin Sun** – Institute of BioPharmaceutical Research, Liaocheng University, Liaocheng City 252059, Shandong Province, China; [orcid.org/0000-0001-5983-7436](https://orcid.org/0000-0001-5983-7436); Email: [goengoy@163.com](mailto:goengoy@163.com)

### Authors

**Yunfei An** – Institute of BioPharmaceutical Research, Liaocheng University, Liaocheng City 252059, Shandong Province, China

**Yue Dong** – Institute of BioPharmaceutical Research, Liaocheng University, Liaocheng City 252059, Shandong Province, China

**Liu Min** – Institute of BioPharmaceutical Research, Liaocheng University, Liaocheng City 252059, Shandong Province, China

**Liyu Zhao** – Key Laboratory of Structure-Based Drug Design & Discovery of Ministry of Education, School of Pharmaceutical Engineering, Shenyang Pharmaceutical University, Shenyang 110016, Liaoning, China

**Dongmei Zhao** – Key Laboratory of Structure-Based Drug Design & Discovery of Ministry of Education, School of Pharmaceutical Engineering, Shenyang Pharmaceutical University, Shenyang 110016, Liaoning, China; [orcid.org/0000-0001-5156-6125](https://orcid.org/0000-0001-5156-6125)

**Jun Han** – Institute of BioPharmaceutical Research, Liaocheng University, Liaocheng City 252059, Shandong Province, China

Complete contact information is available at: <https://pubs.acs.org/doi/10.1021/acsmchemlett.0c00017>

### Funding

The work was supported by the Shandong Provincial Natural Science Foundation (Grant No. ZR2017BH102), the National Natural Science Foundation of China (Grant No. 81703357, Grant No. 21473085), Project of Shandong Collaborative Innovation Center for Antibody Drugs (Grant No. CIC-AD1837), Tai-Shan Scholar Research Fund of Shandong Province of China, and the Open Project of Shandong Collaborative Innovation Center for Antibody Drugs.

## Notes

The authors declare no competing financial interest.

## ■ ABBREVIATIONS

SE, squalene epoxidase; CASE, *Candida albican* squalene epoxidase; BLAST, The Basic Local Alignment Search Tool; SBP, structure-based pharmacophore model; TEM, transmission electron microscopy; LC-MS, liquid chromatography–mass spectrometry

## ■ REFERENCES

- (1) Suleyman, G.; Alangaden, G. J. Nosocomial Fungal Infections: Epidemiology, Infection Control, and Prevention. *Infect. Dis. Clin. North. Am.* **2016**, *30*, 1023–1052.
- (2) Zhao, D.; Zhao, S.; Zhao, L.; Zhang, X.; Wei, P.; Liu, C.; Hao, C.; Sun, B.; Su, X.; Cheng, M. Discovery of biphenyl imidazole derivatives as potent antifungal agents: Design, synthesis, and structure-activity relationship studies. *Bioorg. Med. Chem.* **2017**, *25*, 750–758.
- (3) Kathiravan, M. K.; Salake, A. B.; Chothe, A. S.; Dudhe, P. B.; Watode, R. P.; Mukta, M. S.; Gadhwe, S. The biology and chemistry of antifungal agents: a review. *Bioorg. Med. Chem.* **2012**, *20*, 5678–5698.
- (4) Sun, B.; Huang, W. X.; Liu, M. Evaluation of the combination mode of azoles antifungal inhibitors with CACYP51 and the influence of site-directed mutation. *J. Mol. Graphics Modell.* **2017**, *73*, 157–165.
- (5) Gonzalez Santiago, T. M.; Pritt, B.; Gibson, L. E.; Comfere, N. I. Diagnosis of deep cutaneous fungal infections: Correlation between skin tissue culture and histopathology. *J. Am. Acad. Dermatol.* **2014**, *71*, 293–301.
- (6) Enoch, D. A.; Ludlam, H. A.; Brown, N. M. Invasive fungal infections: a review of epidemiology and management options. *J. Med. Microbiol.* **2006**, *55*, 809–818.
- (7) Calvet, C. M.; Vieira, D. F.; Choi, J. Y.; Kellar, D.; Cameron, M. D.; Siqueira-Neto, J. L.; Gut, J.; Johnston, J. B.; Lin, L.; Khan, S.; McKerrow, J. H.; Roush, W. R.; Podust, L. M. 4-Aminopyridyl-Based Cyp51 Inhibitors as Anti- *Trypanosoma Cruzi* Drug Leads with Improved Pharmacokinetic Profile and in Vivo Potency. *J. Med. Chem.* **2014**, *57*, 6989–7005.
- (8) Yousfi, H.; Ranque, S.; Rolain, J. M.; Bittar, F. In vitro polymyxin activity against clinical multidrug-resistant fungi. *Antimicrob. Resist. Infect. Control.* **2019**, *8*, 66.
- (9) Nalawade, J.; Shinde, A.; Chavan, A.; Patil, S.; Suryavanshi, M.; Modak, M.; Choudhari, P.; Bobade, V. D.; Mhaske, P. C. Synthesis of new thiazolyl-pyrazolyl-1,2,3-triazole derivatives as potential antimicrobial agents. *Eur. J. Med. Chem.* **2019**, *179*, 649–659.
- (10) Moudgal, V.; Sobel, J. Antifungals to treat *Candida albicans*. *Expert Opin. Pharmacother.* **2010**, *11*, 2037–2048.
- (11) Nowosielski, M.; Hoffmann, M.; Wyrwicz, L. S.; Stepniak, P.; Plewczynski, D. M.; Lazniewski, M.; Ginalski, K.; Rychlewski, L. Detailed Mechanism of Squalene Epoxidase Inhibition by Terbinafine. *J. Chem. Inf. Model.* **2011**, *51*, 455–462.
- (12) Sun, B.; Dong, Y.; Lei, K.; Wang, J.; Zhao, L.; Liu, M. Design, synthesis and biological evaluation of amide-pyridine derivatives as novel dual-target (SE, CYP51) antifungal inhibitors. *Bioorg. Med. Chem.* **2019**, *27*, 2427–2437.
- (13) Chen, S. C.; Slavin, M. A.; Sorrell, T. C. Echinocandin antifungal drugs in fungal infections: a comparison. *Drugs* **2011**, *71*, 11–41.
- (14) Papadopoulou, M. V.; Bloomer, W. D.; Lepesheva, G. I.; Rosenzweig, H. S.; Kaiser, M.; Aguilera-Venegas, B.; Wilkinson, S. R.; Chatelain, E.; Ioset, J. R. Novel 3-nitrotriazole-based amides and carbinols as bifunctional antichagasic agents. *J. Med. Chem.* **2015**, *58*, 1307–1319.
- (15) Zhao, S.; Zhao, L.; Zhang, X.; Liu, C.; Hao, C.; Xie, H.; Sun, B.; Zhao, D.; Cheng, M. Design, synthesis, and structure-activity relationship studies of benzothiazole derivatives as antifungal agents. *Eur. J. Med. Chem.* **2016**, *123*, 514–522.
- (16) Moudgal, V.; Sobel, J. Antifungals to treat *Candida albicans*. *Expert Opin. Pharmacother.* **2010**, *11*, 2037–2048.
- (17) Zhao, D.; Zhao, S.; Zhao, L.; Zhang, X.; Wei, P.; Liu, C.; Hao, C.; Sun, B.; Su, X.; Cheng, M. Discovery of biphenyl imidazole derivatives as potent antifungal agents: Design, synthesis, and structure-activity relationship studies. *Bioorg. Med. Chem.* **2017**, *25*, 750–758.
- (18) Sun, B.; Zhang, H.; Liu, M.; Hou, Z.; Liu, X. Structure-based virtual screening and ADME/T-based prediction analysis for the discovery of novel antifungal CYP51 inhibitors. *MedChemComm* **2018**, *9*, 1178–1187.
- (19) Fiser, A.; Sali, A. Modeller: generation and refinement of homology-based protein structure models. *Methods Enzymol.* **2003**, *374*, 461–491.
- (20) Padyana, A. K.; Gross, S.; Jin, L.; Cianchetta, G.; Narayanaswamy, R.; Wang, F.; Wang, R.; Fang, C.; Lv, X.; Biller, S. A.; Dang, L.; Mahoney, C. E.; Nagaraja, N.; Pirman, D.; Sui, Z.; Popovici-Muller, J.; Smolen, G. A. Structure and inhibition mechanism of the catalytic domain of human squalene epoxidase. *Nat. Commun.* **2019**, *10*, 97.
- (21) Eisenberg, D.; Lüthy, R.; Bowie, J. U. VERIFY3D: assessment of protein models with three-dimensional profiles. *Methods Enzymol.* **1997**, *277*, 396–404.
- (22) Sun, B.; Huang, W.; Liu, M.; Lei, K. Comparison and analysis of the structures and binding modes of antifungal SE and CYP51 inhibitors. *J. Mol. Graphics Modell.* **2017**, *77*, 1–8.
- (23) Kuntz, I. D. Structure-based strategies for drug design and discovery. *Science* **1992**, *257*, 1078–1082.
- (24) Chen, S. H.; Sheng, C. Q.; Xu, X. H.; Jiang, Y. Y.; Zhang, W. N.; He, C. Expression and detection the enzyme activity of the wild and mutation type of CYP51 protein of *Candida albicans*. *Microbiology.* **2009**, *36*, 1564–1570.
- (25) Chandrika, N. T.; Shrestha, S. K.; Ngo, H. X.; Garneau-Tsodikova, S. Synthesis and investigation of novel benzimidazole derivatives as antifungal agents. *Bioorg. Med. Chem.* **2016**, *24*, 3680–3686.
- (26) Dong, Y.; Liu, M.; Wang, J.; Ding, Z.; Sun, B. Construction of antifungal dual-target (SE, CYP51) pharmacophore models and the discovery of novel antifungal inhibitors. *RSC Adv.* **2019**, *9*, 26302–26314.
- (27) Dong, Y.; Liu, X. Y.; An, Y. F.; Liu, M.; Han, J.; Sun, B. Potent arylamide derivatives as dual-target antifungal agents: Design, synthesis, biological evaluation, and molecular docking studies. *Bioorg. Chem.* **2020**, *99*, 103749.
- (28) Sun, B.; Zhang, H.; Dong, Y.; Zhao, L.; Liu, M. Evaluation of the combination mode and features of p38 MAPK inhibitors: construction of different pharmacophore models and molecular docking. *Mol. Simul.* **2019**, *45*, 975–984.
- (29) Cao, X.; Xu, Y.; Cao, Y.; Wang, R.; Zhou, R.; Chu, W.; Yang, Y. Design, synthesis, and structure-activity relationship studies of novel thienopyrrolidone derivatives with strong antifungal activity against *Aspergillus fumigates*. *Eur. J. Med. Chem.* **2015**, *102*, 471–476.